Chlorophyll Triplet States Associated with Photosystem II of Thylakoids†

Stefano Santabarbara,*,‡,§ Enrica Bordignon,|| Robert C. Jennings,‡ and Donatella Carbonera||

Centro C.N.R. Biologia Cellulare e Molecolare delle Piante, Dipartimento di Biologia, Università di Milano, Via Celoria 26, 20100, Milano, Italy, and Dipartimento di Chimica Fisica, Università di Padova, Via Loredan 2, 35131, Padova, Italy

Received February 8, 2002; Revised Manuscript Received April 25, 2002

ABSTRACT: The analysis of FDMR thylakoid spectra, determined at multiple emission wavelengths, by a global decomposition technique, has revealed the presence of three previously undescribed triplet populations at emission wavelengths characteristic of Photosystem II chlorophyll/protein complexes. Their zero-field splitting parameters have been determined in order to compare them with the well-studied PSII recombination triplet state. None of these triplets have the zero-field splitting parameters characteristic of the recombination triplet and are therefore probably not generated directly in the reaction center. On the basis of their microwave-induced emission spectra, it is suggested that two are probably generated in the core complex(es) while the third may be generated in the external antenna. These triplets are formed under nonreducing redox conditions, when the recombination triplet is undetectable. It is suggested that they may be involved in the photoinhibitory damage of Photosystem II. The triplet-minus-singlet spectrum associated with the recombination triplet state has been determined for thylakoids after reduction of the secondary acceptors. Its main peak is at 685 nm, slightly red shifted with respect to earlier reports, with a weak signal, of opposite sign at approximately 675 nm. The 685 nm peak indicates that at cryogenic temperatures, the triplet is located on the long-wavelength chlorophyll state present in the reaction center complex of Photosystem II (D1·D2·Cytb_{559} complex). From the absence of a clear structure in the 680 nm absorption region, this long-wavelength absorbing state does not appear to be strongly coupled to P_{680}, though it must be associated with one of the "inner core" pigments recently identified in the photosystem II crystallographic structure [Zouni et al. (2001) *Nature 408*, 739−743].

Thylakoids are the site where the primary events of photosynthesis, associated with light absorbance and its conversion into chemical energy, take place. Two photosystems, namely, Photosystem II (PSII) and PSI, operate in series transferring electrons from water to NADP against the electrochemical gradient. The photosystems are large multisubunit complexes which bind a number of different classes of cofactors. In the past few years, it has been possible to obtain structural information for both the photosystems by means of X-ray diffraction (*1*−*3*) and cryoelectron microscopy (*4*−*6*) crystallographic techniques. Despite the great differences at the level of the polypeptide composition, the two photosystems seem to be arranged in a similar fashion around a special pair (i.e., *7*−*9*), or cluster (i.e., *10*, *11*), of chlorophyll molecules which are able to perform a charge-separation reaction (the reaction centers). The direct excitation of the RC is a rare event, and excitation is efficiently transferred to the trap from the large antenna pigment matrixes. PSII has a complicated arrangement with the Chl *a*/*β*-carotene binding inner antenna complexes, CP43 and CP47, apparently located on either side of the D1·D2 heterodimer, which coordinates the primary electron donor Chls, known as P_{680}, and the primary acceptor pheophytin (Pheo or I). In the case of PSI, it is the gene products of the *psa*A and *psa*B genes that act both as the inner antenna, coordinating about 100 Chl *a* and about 30 *β*-Car molecules, and the reaction center, binding the primary donor, P_{700}, as well as the primary electron acceptors, A_0 and A_1. In higher plants, the outer antenna complexes of PSI (LHCI pool) and PSII (LHCII pool) bind Chl *a*, Chl *b*, and xanthophylls (see ref *12* for a review).

In plant photosystems, excitation energy transfer from the antenna to the primary donors, as well as primary charge separation, occurs at the level of the lowest-lying chlorophyll singlet excited state and is highly efficient when the primary donors are in the appropriate redox state. Thus, the Chl triplet, which in solvated chlorophyll has a yield of around 60% (see ref *13* for a review), is of little direct importance in photosynthetic energy conversion. However, it has been

† This work was in part supported by the MURST project "Fotoinibizione: meccanismi molecolari e meccanismi di protezione", n. 97051500_004, the CNR target protein on Biotechnology, and the TMR program "Molecular Mechanism of Photosynthetic Energy Conversion" C.N. ERBFMRXCT98-0214.

* Corresponding author. Address: Please use Queen Mary and Westfield address. Phone: 044-020-7882-3019. Fax: 0044-020-8983-0973. E-mail: s.santabarbara@qmul.ac.uk.

‡ Centro C.N.R. Biologia Cellulare e Molecolare delle Piante.

§ Present Address: School of Biological Science, Queen Mary and Westfield College, University of London, London 1N 4NS, United Kingdom.

|| Università di Padova.

[1] [1]Abbreviations: Chl, chlorophyll; DCMU, 3-(3,4-dichlorophenyl)-1,1-dimethyl-urea; ODMR, optically detected magnetic resonance, FDMR fluorescence-detected magnetic resonance; ADMR absorbance-detected magnetic resonance; EPR, electronic paramagnetic resonance; EEDOR, electron electron double resonance; ZFS, zero-field splitting; T − S, triplet-minus-singlet difference absorption spectrum; RC, reaction center; LHC light-harvesting complex; PSII, Photosystem II; PSI, Photosystem I; P_{680}, Photosystem II primary donor; P_{700}, Photosystem I primary donor; isc, intersystem crossing; fwhm full width at half-maximum; F_M, maximal fluorescence yield of Photosystem II.

10.1021/bi0201163 CCC: $22.00
Published on Web 05/18/2002

known for some time that Chl triplets probably have a primary role in the induction of light stress phenomena, known as photoinhibition. This is because of their interaction with molecular oxygen, which generates the highly oxidizing singlet oxygen species (see ref *14* for a review). Chl triplet states may be populated in principle either by intersystem crossing (isc) from any singlet excited state or by the recombination of the charge separated $[P^+I^-]$ state of the reaction center. The rate of intersystem crossing, in isolated protein−pigment complexes, is significant and on the same order of magnitude as that for the other trivial decay process (*15*). Within the photosystems, Chl triplet levels are efficiently quenched by carotenoids (e.g., *15*−*19*). Nevertheless, Chl triplets have been detected in many PSII enriched particles (*17*) and components, including outer (*20*−*22*) and inner antenna (*23*, *24*) complexes, though it is not known whether these triplets are also formed in intact systems.

The Chl triplet formed by charge recombination at both PSI and PSII reaction centers has received considerable attention over the past decades in an attempt to gain structural information. Thus, a spin-polarized Chl triplet in PSI enriched particles was initially reported by Bearden and Malkin (*25*), and its charge recombination mechanism was demonstrated afterward (*26*−*28*). The PSII reaction center recombination triplet, initially detected by Rutherford and Mullet (*29*), is significantly populated only when the quinone acceptor Q_A is doubly reduced and in the uncharged Q_AH_2 form (*30*).

As mentioned above, it is well known that the Chl triplet interacts with molecular oxygen to form singlet oxygen which produces photoinhibitory damage, principally at the level of PSII. This has been attributed to the PSII recombination triplet (*31*, *32*), which has been suggested to form under conditions of saturating light intensity (*32*). However, recent studies have provided strong evidence that much light-induced damage in isolated thylakoids and intact algal cells occurs via Chls which are energetically uncoupled from the main antenna matrix (*33*−*35*), and it was hypothesised that these chlorophylls, possibly associated with damaged or incompletely assembled PSII antenna complexes, may have a high triplet yield. We have therefore searched for the presence of Chl triplet populations in isolated thylakoids, which are not associated with charge recombination, using the FDMR technique, which is highly sensitive and which also has the advantage of selectivity over the emission wavelength. At least three PSII triplet populations are shown to be present and are characterized with respect to their zero-field splitting parameters and microwave-induced fluorescence emission dependence. These triplets are detected in aerated samples, though with Q_A singly reduced, conditions in which the P_{680} recombination triplet is not detected.

EXPERIMENTAL PROCEDURES

Thylakoids were prepared from freshly harvested spinach leaves as previously described (*36*). The chlorophyll concentration was estimated from the 80% acetone extract by the absorption coefficients given by McKinney (*37*). All chemical additions were made in alcohol, and the final V/V ratio never exceeded 1%. Anaerobiosis was obtained by means of the glucose/glucose-oxidase/catalase system. Extra pure glycerol was added to the sample to a final 60:40 V/V ratio immediately before the sample was placed in the cryostat.

Steady-State Fluorescence Spectroscopy. Steady-state fluorescence emission spectra were detected in a home-built fluorimeter equipped with an EG&G OMAIII (model 1460) with an intensified diode array detector mounted on a HR320 Jobin-Ivon spectrometer and adapted to fit a continuous helium flow cryostat (Oxford Instruments Model Optistat^{CF}). The temperature of the sample was monitored by a thermocouple placed in the sample and controlled with an ITC-503 device (Oxford Instruments). The wavelength scale was calibrated using a neon spectral calibration source (Cathodeon). Excitation wavelengths were selected by a Heath monochromator and two Corning CS 4-96 broad band-pass filters and, unless otherwise stated, was fixed to 435 nm. The light path was 1 cm. To have an adequate signal-to-noise ratio, we accumulated spectra to around 10^5 counts at the emission maxima. All spectra were measured at a chlorophyll concentration of 4 μg/mL. Spectra were corrected for the detector sensitivity as previously described (*38*).

Optically Detected Magnetic Resonance Apparatus. For the ODMR measurements, the microwave source was an HP8559b sweep oscillator equipped with the HP83522a plug-in device (0.01−2.4 GHz). The microwave were amplified by a LogMetrics A210/L TWT amplifier in the range of 1−2 GHz and by a Sco-Nucletudes 10-46-30 TWT amplifier in the 0.01−1 GHz range and transmitted trough a semirigid coaxial cable to the sample held in a slow-wave helix with a pitch of about 2 mm. The experiments were performed with a maximum output power of 600 mW. The microwaves were amplitude modulated with a square waveform from a Wavetek signal generator (mod. 164), at frequency between 20 and 1000 Hz. Optical excitation was provided by a tungsten lamp (Philips 250W supplied by a Oltronix B 32-20R power supply). For the fluorescence-detected experiments (FDMR), the light, filtered through an 8 cm wide 0.1 M $CuSO_4$ solution and a 630 nm cut on filter (Ealing), was focused by a 10 cm diameter lens with a 10 cm focal length onto a flat cell (5,0 × 1,0 mm) placed in a liquid helium cryostat (Oxford instruments, mod. Spectromag 4) which can be pumped to reach the temperature of 1.25 K. The sample was kept with the normal to its plane rotated 40° about the cryostat axis, and the emission was collected at 90° through interference filters (fwhm 10−15 nm), with an OSI 5K (Centronic) photodiode. The signal was detected with a phase-sensitive lock-in amplifier (EG&G mod. 5210), interfaced to a PC by a software written in the laboratory (*23*). The same apparatus was adapted to perform the absorption detection, ADMR experiments: the beam was filtered through a 5 cm water path-length and a cut-on 575 nm (Coherent Ealing) and was focused on the flat cell (1 mm width) placed perpendicular to the light beam. The transmitted light was analyzed by a Jobin-Ivon HR250 monochromator, protected by a cut-on filter OG 550 (Schott), equipped with the Data-Link device controlled by a PC, and acquired by the same photodiode used for the fluorescence experiments. The photodiode voltage output is phase-sensitive and was detected with an EG&G mod 5210 lock-in amplifier and presented as the ratio of amplitude modulated and continuous components ($\Delta I/I$). For fluorescence-detected resonance measurements (FDMR), the sample was diluted to a concentration of 100 μg/mL Chl, which was reduced to

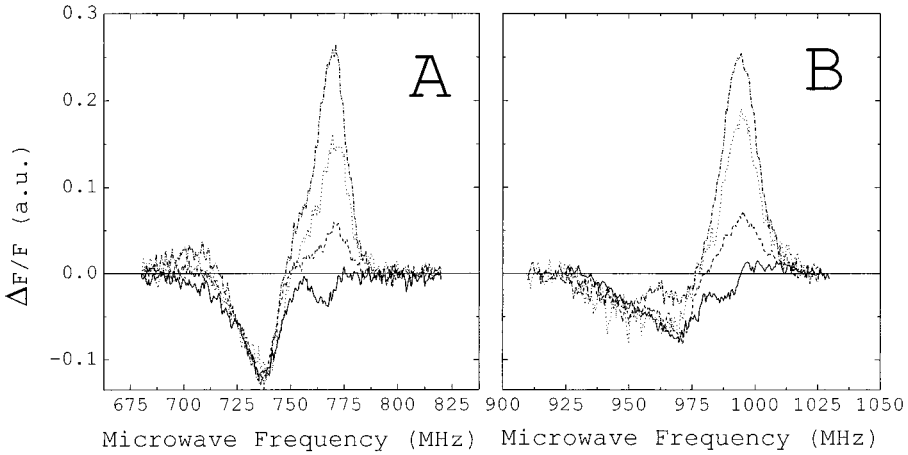

FIGURE 1: Effect of dark incubation of thylakoids with glycerol (60:40 V/V) at 4 °C on FDMR spectra recorded in the |D| − |E| (panel A) and |D| + |E| (panel B) Chl *a* resonance transitions. Preincubation time: 0′, solid line; 45′, dashed line; 90′, dotted line; 120′, dash−dotted line. λ_{em}, 690 nm (fwhm 10 nm); temperature, 1.8 K; Mw mod. freq., 33 Hz; lock-in ϕ, −105°; Mw power, 600 mW; scan rate, 5 MHz/sec.

40 μg/mL for ADMR and the microwave-detected triplet-minus-singlet (T − S) experiments.

Upon illumination, the fluorescence signal at 1.8 K is strongly quenched and reaches a constant value after about 5 min, which is about 60−65% of the initial value. Quenching of PSII fluorescence at low temperature has been previously reported at 77 K and correlated to the accumulation of an accessory chlorophyll cation (*39*, *40*). The FDMR spectra were acquired after the steady state was reached.

Induction of the P_{680} recombination triplet was obtained by illumination at room temperature of dithionite-incubated (20mM) samples at a Chl concentration of 100 μg/mL in a 1.5 mm path-width cuvette, with a 150 W tungsten lamp, filtered by a 5 cm water filter and a heat mirror (Ealing 35−6865). The intensity was 2000 μEinstein m^{-2} s^{-1}. After the room temperature illumination, samples were immediately transferred to the cryostat, precooled at 40 K.

Deconvolution Analysis of Fluorescence Emission and FDMR Spectra. Deconvolution analysis in terms of Gaussian subbands of the fluorescence emission spectra was performed using a software developed in the laboratory running over a Digital VAX-workstation, as previously described (*41*).

The |D| + |E| and |D| − |E| resonance lines of the FDMR spectra, recorded at multiple emission wavelengths, were simultaneously fitted, using a global procedure based on a symmetrical Gaussian function. The microwave frequency of the Gaussian maxima and bandwidths were fit parameters and were constrained to remain constant for the different spectral series (|D| + |E| or |D| − |E|). Amplitudes were allowed to change with corresponding bands in the |D| + |E| and |D| − |E| being coupled. To take into account the differences in the signal-to-noise levels between the microwave spectra recorded at different emission wavelengths, we recorded at each wavelength the spectra of the sample in a microwave region that did not induce triplet sublevel resonance and estimated the error as the root-mean-square noise over the average output component, weighted for the number of scans. The FDMR spectra were globally deconvoluted using a software developed in collaboration with Tommaso Tagliabue, in which the sum of $\chi^2(\lambda_{em})$ was minimized by a Levenberg−Marquard non-linear least-squares algorithm.

RESULTS AND DISCUSSION

Thylakoid Triplet Populations. In the following, we present a detailed characterization of the chlorophyll triplet populations in freshly isolated thylakoid membranes by means of the FDMR technique. Care was taken to use freshly prepared thylakoids and to avoid prolonged incubation of samples with the cryoprotectant, glycerol, as this leads to artifactual triplet production, probably due to the uncoupling of a small fraction of the protein-bound Chls. An example of this is shown in Figure 1 for the |D| − |E| and |D| + |E| transitions where prolonged incubation of thylakoids in ice, with glycerol, can be seen to bring about the formation of triplet populations with resonance maxima between 750−775 MHz and 980−1015 MHz, respectively. Triplet signals with similar characteristic have often been reported using different isolated particles and complexes in FDMR experiments (e.g., *42*−*45*). No 2|E| transitions have been detected, as commonly found for Chl triplet states.

In Figure 2, the FDMR spectra of untreated samples, recorded at emission wavelengths ranging from 680 to 760 nm, are presented in the Chl *a* |D| − |E| (680−820 MHz) and |D| + |E| (910−1010 MHz) resonance lines. The upper traces in Figure 2 describe the FDMR spectra in the wavelength region in which fluorescence is essentially emitted by PS I (720−760 nm). The spectra do not change significantly up to 800 nm (data not presented). Spectra recorded in the |D| − |E| transition show a broad, asymmetric peak at about 725−730 MHz, suggesting that it originates from a contribution of at least two components. The heterogeneity of the FDMR signal components is less evident in the |D| + |E| line (max. at 940 MHz), although some asymmetry on the low frequency side is also present. These data, using thylakoids, are in close agreement with those previously reported for isolated PSI-200 particles and thylakoids (*45*) and have been assigned to PSI reaction center recombination triplets, with the $^3P_{700}$ being frozen in two different conformational configurations. The T − S spectrum of these signals (data not presented) confirms their origin in P_{700}.

When fluorescence is detected at wavelengths dominated by PSII emission, the FDMR spectra show two main structures in both the magnetic transitions investigated:

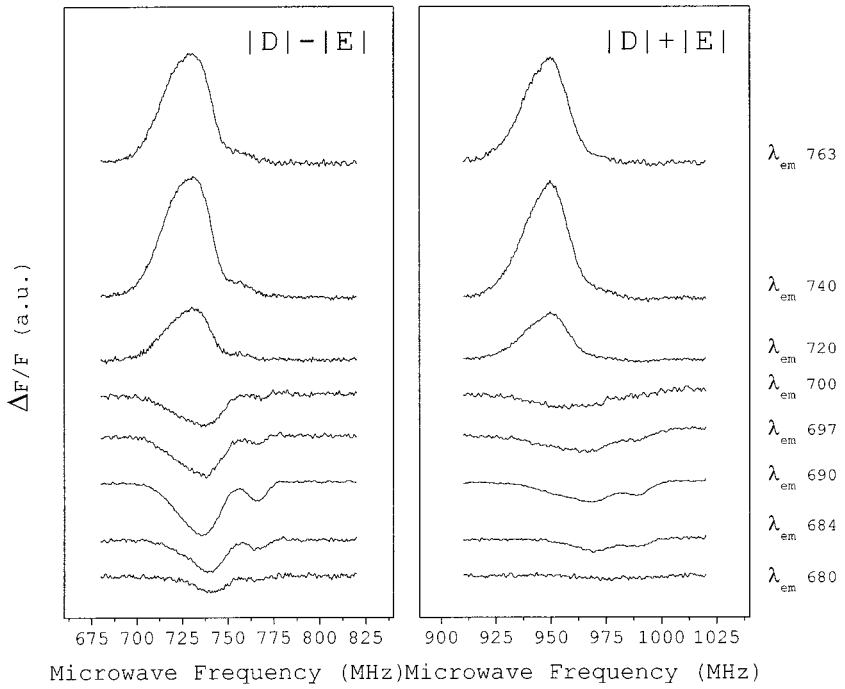

FIGURE 2: FDMR spectra of thylakoids in the |D| − |E| (panel A) and |D| + |E| (panel B) transitions measured at multiple emission wavelengths in the 680−763 nm interval. The optical bandwidth of interference filters were about 10 nm (fwhm). Temperature, 1.8 K; Mw mod. freq., 33 Hz; lock-in ϕ, −105°; Mw power, 600 mW; scan rate, 5 MHz/sec. Spectra are offset for clarity.

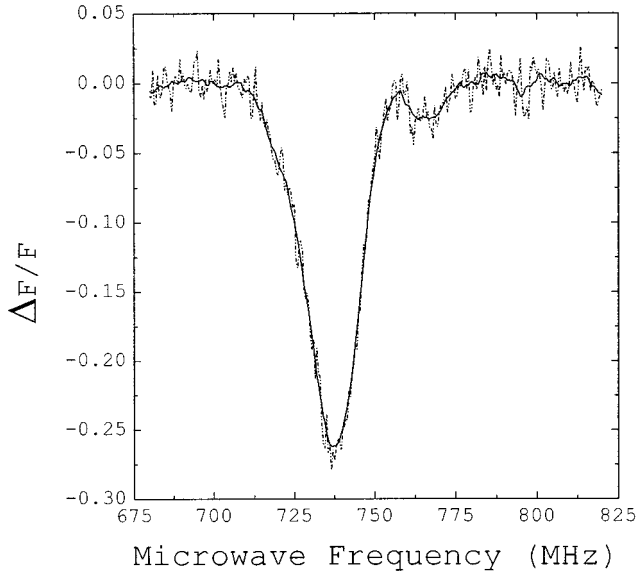

FIGURE 3: FDMR spectra of spinach leaves in the |D| − |E| transition recorded at the emission wavelength of 690 nm (dash−dotted line). Also presented is the smoothed spectrum (solid line). Temperature, 1.8 K; Mw mod. freq., 33 Hz; lock-in ϕ, −105°; Mw power, 20mW; scan rate, 5 MHz/sec.

(i) a sharp (fwhm ≈ 13 MHz) peak at 766 ± 0.5 MHz (|D| − |E|) and 989 ± 0.5 MHz (|D| + |E|), and
(ii) a rather broad (fwhm 30−35 MHz) and asymmetric band peaking at about 734−736 MHz (|D| − |E|) and 968−970 MHz (|D| + |E|).

We have checked that these signals in the PSII emission region are not induced by the preparation of thylakoids or by the limited contact of thylakoids with glycerol, by examining the |D| − |E| microwave spectrum for spinach leaves at 690 nm (Figure 3). While there is clearly a decrease of the signal-to-noise ratio for the leaf measurement, it is evident that the spectrum is similar to that of thylakoids.

The sharpness of the 766/989 MHz structure, which is much more evident in the |D| − |E| line, indicates that this triplet originates from a single and rather homogeneous population of molecules. On the other hand, in the short microwave region of both lines, the broadness, as well as the changes in symmetry as a function of the detection wavelength, indicates that multiple, overlapping contributions are present. Data on Chl triplets with these microwave characteristics have not been previously published. We have attempted to determine the T − S spectra of these triplet populations using ADMR. These attempts however were unsuccessful due to the weakness of the signals.

To gain further information on these triplets, we have performed a series of experiments employing triplet lifetime selection, by means of the phase suppression technique. The signals presented in Figure 2 were recorded at a phase angle of −105° and a microwave field frequency modulation of 33 Hz, optimized on the 734 MHz signal. This corresponds to a triplet lifetime in the range of 1−2 ms, which is a typical range of values reported for the Chl triplet lifetime (e.g., *7*, *8*, *13*, *17*, *21*, *22*, *31*, *46*). On the other hand the data presented in Figure 4 were recorded at a higher modulation frequency of the microwave field (320 Hz), optimized on the 766 MHz component. The large changes in overall microwave spectral shape at PSII emission wavelengths, with a pronounced increase in the 766/989 MHz component, indicate that this triplet has a lifetime of 50−150 μs. This is an unusually fast decay for a Chl triplet. This measurement also confirms the assignment of the 989 MHz signal as the |D| + |E| resonance transition of the 766 MHz |D| − |E| transition. It will also be noticed that the band shape of the 730−740 MHz (|D| − |E|) component of Figure 2 is modified under the higher modulation frequency conditions used for the measurements of Figure 4. This is shown more clearly in Figure 5, where the spectra, measured at 690 nm

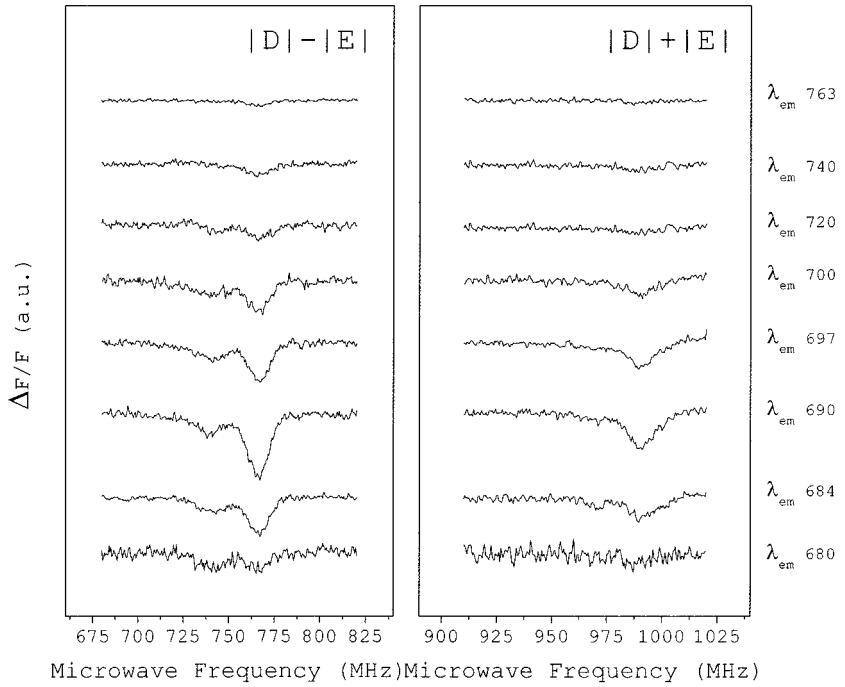

FIGURE 4: FDMR spectra of thylakoids in the |D| − |E| (panel A) and |D| + |E| (panel B) transitions recorded at multiple emission wavelengths in the 680−763 nm interval, using a microwave field modulation frequency of 320 Hz. Temperature, 1.8 K; Mw mod. freq., 320 Hz; lock-in ϕ, 12°; Mw power, 600 mW; scan rate, 5 MHz/sec. Spectra are offset for clarity.

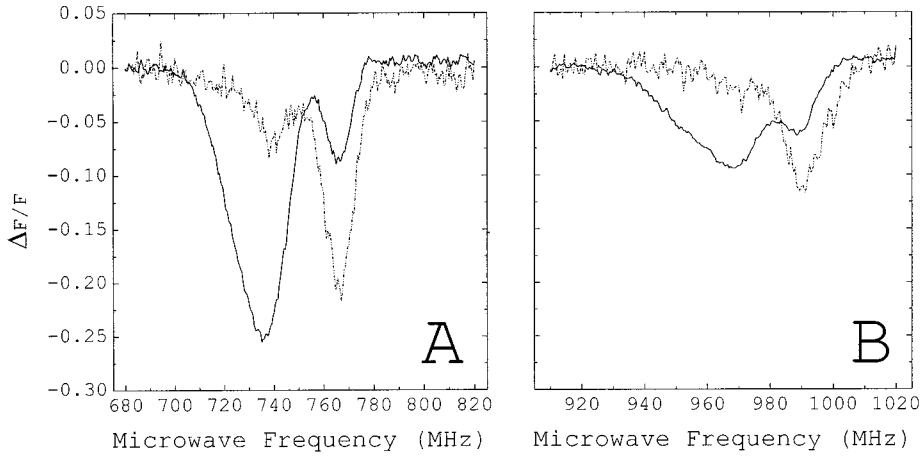

FIGURE 5: Comparison of the FDMR spectra of thylakoids in the |D| − |E| (panel A) and |D| + |E| (panel B) transitions recorded at the microwave field modulation frequencies of of 33 Hz (ϕ, −105°; solid lines) or 320 Hz (ϕ, 12°; dash−dotted lines); λ_{em}, 690 nm (fwhm 10 nm); temperature, 1.8 K; Mw power, 600 mW; scan rate, 5 MHz/sec.

for both modulation frequencies, are directly compared. At the higher modulation frequency, the 730−740 MHz band becomes more symmetrical and maximal at 740 MHz for the |D| − |E| transition. This clearly indicates the presence near 730 MHz (|D| − |E|) of another triplet population, which is only detected at the 33 MHz modulation frequency. It can also be seen in Figure 5 that the 740 MHz |D| − |E| transition is associated with an approximately 970 MHz transition in the |D| + |E| region. These measurements, at different modulation frequency, thus clearly identify the |D| − |E| and |D| + |E| transitions of two distinct triplet populations in the PSII emission region and indicate the presence of a third triplet population on the short microwave side of both the |D| − |E| and |D| + |E| transitions. These assignments of corresponding |D| − |E| and |D| + |E| transitions were also confirmed by double resonance experiments of the kind presented in Figure 6. Interestingly, the signal originating from PSI is almost completely suppressed under the measurement conditions of Figure 4, indicating that these are longer (ms) lifetime triplet populations.

Global Decomposition of FDMR Spectra. To untangle the different and often overlapping triplet signals in thylakoids, we have analyzed the collection of FDMR spectra recorded at multiple emission wavelengths and microwave field modulation frequencies by a global decomposition procedure based on a Gaussian band shape. The use of Gaussians is justified because at the low temperatures of the experiments the band-shape is essentially determined by the inhomogeneous site distribution of the triplet sublevels (*47*, *48*). While the position of the Gaussian maxima and fwhm were free fit parameters, their values were constrained to remain constant by the global routine over the wavelength and phase-

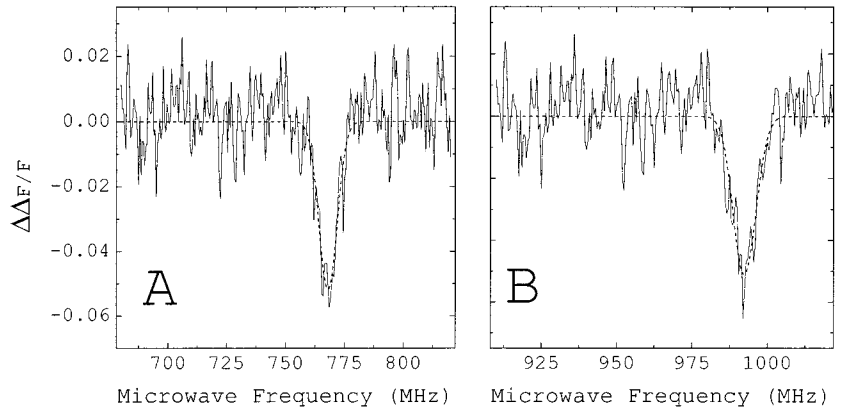

FIGURE 6: Electron electron double resonance (EEDOR) spectra of thylakoids. Presented are holes burned in the |D| − |E| (panel A) and |D| + |E| (panel B) transitions recorded at the microwave burning frequency of 766 MHz (Mw power, 600 mW) and modulation frequency of 33 Hz (lock-in phase: ϕ, −105°). Also shown are the fits with a single Gaussian component (dashed lines). λ_{em}, 690 nm (fwhm, 10 nm); temperature, 1.8 K; Mw power, 20mW; scan rate, 5 MHz/sec.

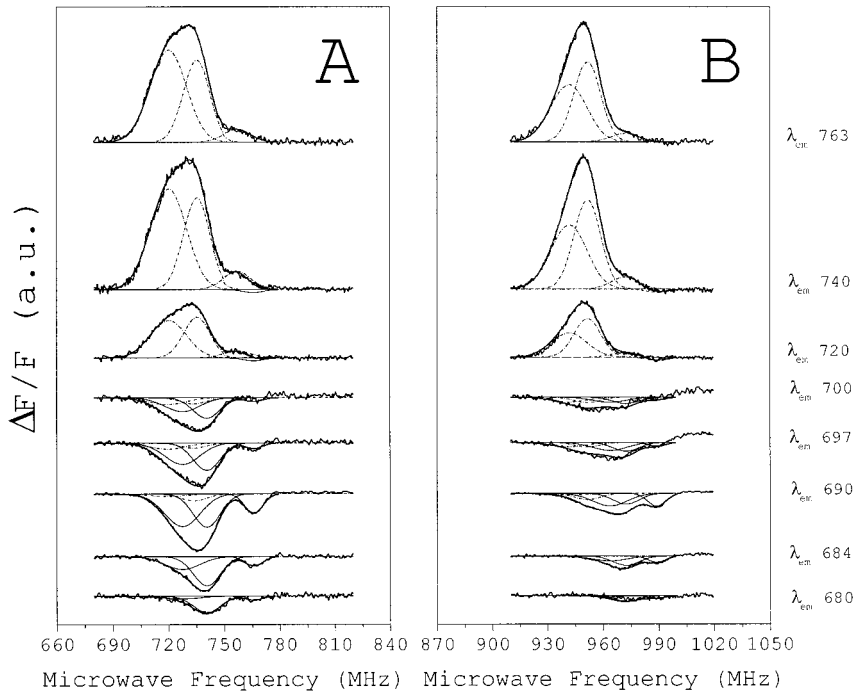

FIGURE 7: Global Gaussian deconvolution of FDMR spectra of thylakoids in the |D| − |E| (panel A) and |D| + |E| (panel B) transitions at multiple emission wavelengths in the 680−763 nm interval recorded with a 33 Hz microwave modulation frequency. Measured spectra (solid lines), fit function (thick solid lines). Gaussian sub-bands associated with PSII are solid lines, and those associated with PSI are dash−dotted lines. Conditions same as those in the legend of Figure 2.

frequency modulation windows used. The amplitudes were allowed to vary though a constant amplitude scaling factor connecting the |D| − |E| and |D| + |E| transition. This scaling factor was determined by the fit procedure. The global description of the experimental data is presented in Figures 7 and 8, and the details of the fit parameters, together with relative zero-field splitting (ZFS) parameters, are given in Table 1. To satisfactorily describe the data, six subbands are required, for which the ZFS parameters are all within the range of values reported in the literature for solvated and protein-bound Chl. Of these, the 719.9/942 and 733/951 MHz sub-bands are attributed to P_{700}, following Searle and Schaafsma (*43*) and Carbonera et al. (*45*). They are also present in some of the lower-wavelength spectra (690−700 nm), though as minor bands of opposite sign. This point is more clearly apparent in Figure 9 and has been attributed to energy transfer from these shorter-wavelength Chls to P_{700} (*43*, *45*). The 757.2/972.3 MHz triplet, also associated with PSI on the basis of the fluorescence detection wavelength (Figure 7), has not been previously noticed.

In the PSII emission region, three additional sub-bands are required at 727.7/964, 740.8/972, and 766/989 MHz. None of these triplet populations have been unambiguously reported in previous studies, as far as we are aware. While both the 727.7/964 and 740.8/972 MHz triplets have millisecond lifetimes, the 766/989 MHz triplet has a microsecond lifetime. The sub-band associated with this triplet is narrow (fwhm 13.5 MHz), indicating a smaller inhomogeneous distribution with respect to the others. The microwave-induced fluorescence emission spectrum associated with all three triplets, obtained by a plot of the subband amplitudes versus the peak transmission maximum of the emission filter,

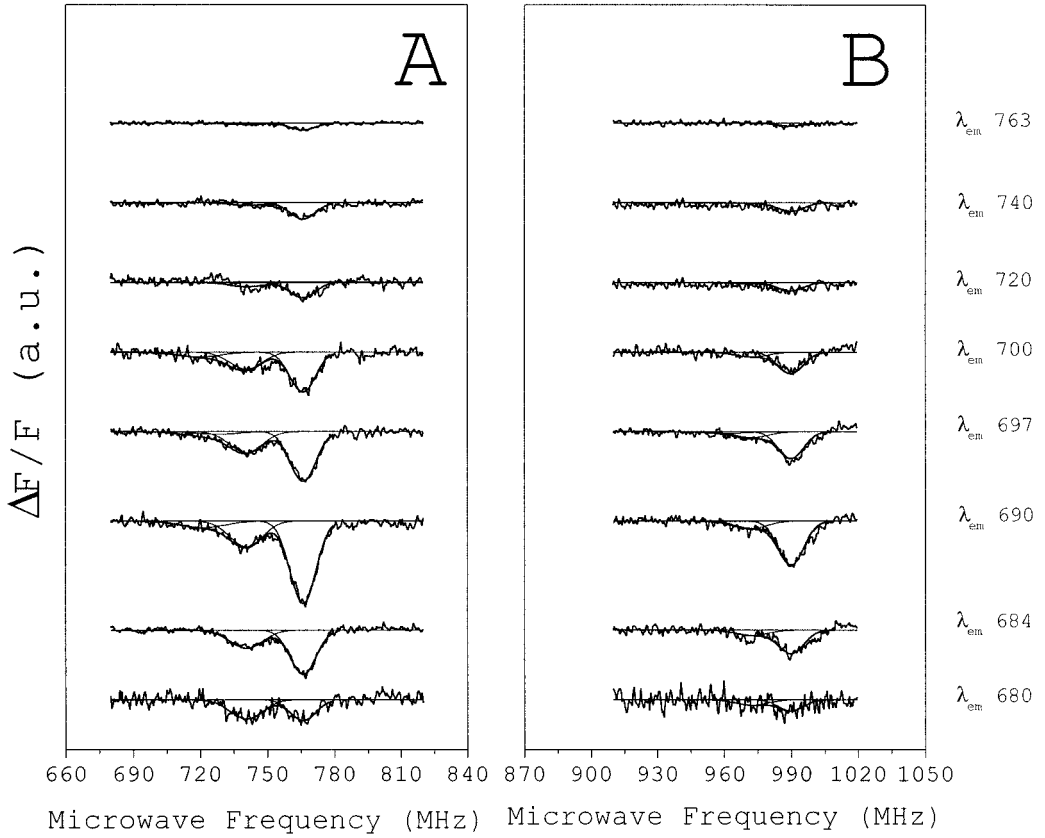

FIGURE 8: Global Gaussian deconvolution of FDMR spectra of thylakoids in the |D| − |E| (panel A) and |D| + |E| (panel B) transitions at multiple emission wavelength in the 680−763 nm interval recorded with a 320 Hz microwave modulation frequency. Measured spectra (solid lines), fit function (thick solid lines). Gaussian sub-bands associated with PSII, are solid lines and those associated with PSI are dash−dotted lines. Condition same as those in the legend of Figure 3.

Table 1: Parameters of Global Gaussian Decomposition of FDMR Spectra of Thylakoids[a]

triplet	|D| − |E| (MHz)	|D| + |E| (MHz)	fwhm (MHz)	|D| (cm^{-1})	|E| (cm^{-1})	assignment
T_{PSI}^1	719.9	942.0	23.0	0.0277	0.0037	$^3P_{700}$
T_{PSI}^2	733.0	951.0	16.7	0.0281	0.0036	$^3P_{700}$
T_{PSI}^3	757.2	972.3	17.4	0.0288	0.0037	
T_{PSII}^1	727.7	964.0	22.0	0.0282	0.0039	PSII core antenna
T_{PSII}^2	740.8	972.0	17.4	0.0286	0.0037	PSII core antenna/ PSII outer antenna
T_{PSII}^3	766.0	989.0	13.5	0.0292	0.0037	PSII core antenna
T_{PSII}^4	720.5	991.0	14.7	0.0285	0.0045	$^3P_{680}$

[a] In Table 1 are reported the value of maxima and the width of Gaussian functions employed in the global deconvolution analysis of FDMR spectra of thylakoids monitored at multiple emission wavelengths. Also indicated are the zero-field splitting parameters |D| and |E|. Errors are ±0.0001 cm^{-1}.

has a clear maximum at 690 nm (Figure 9B). The 766/989 MHz triplet has a somewhat broader emission selectivity than the other two.

To further analyze the emission selectivity of the three PSII triplets, we have measured the steady-state emission spectra of thylakoids at 4.2 K (Figure 10). The spectrum, maximal at 692 nm, is clearly structured near 680 and 687 nm, as seen in the second derivative spectrum (data not shown) and as reported by Rijgersberg at al. (*49*) for this temperature. Gaussian decomposition describes these structures with three major subbands at 682, 687, and 693 nm (Figure 10). The long-wavelength, markedly asymmetric subband represents mainly vibrational transitions and a minor band near 675 nm is also present. The 680 and 687 nm subbands have a fwhm of approximately 130−140 cm^{-1}, consistent with the inhomogeneous width of single antenna pigments (*50*, *52*). On the other hand, the 693 nm subband is broader (fwhm = 210 cm^{-1}) and is therefore probably composite in origin. From an analysis of the *chlorina* f_2 barley mutant lacking the external antenna complexes, Rijgersberg et al. (*49*) concluded that the 680 nm emission is associated with the external antenna components and the longer-wavelength emission bands with the PSII core. If this assignment is correct, it would appear that the terminal emitter(s) of the three PSII triplet populations are associated with the core (Figure 9B,C). This, however, does not necessarily mean that the triplets are generated in the core complexes as efficient energy transfer from the external antenna complexes to the core complexes is demonstrated by the low yield of the external antenna complexes emission (680 nm band) at this temperature. This situation is schematically represented in the model (Figure 11). As the transfer rate from the external antenna to the core (k_1) must be greater than that for transfer from the external antenna to its own terminal emitter (k_2), it is easily shown that triplets may be generated in the external antenna complexes and have an FDMR maximum at core emission wavelengths. However, in this case, it is expected that the fluorescence in the 680−685 nm region will be relatively greater than that for triplets generated in the core complexes themselves. Such a difference is indeed seen in Figure 9 for the 740.8/972 MHz triplet with respect to both the 727.7/964 and 766/989 MHz triplets. Thus, we suggest that the 740.8/972 MHz triplet may be

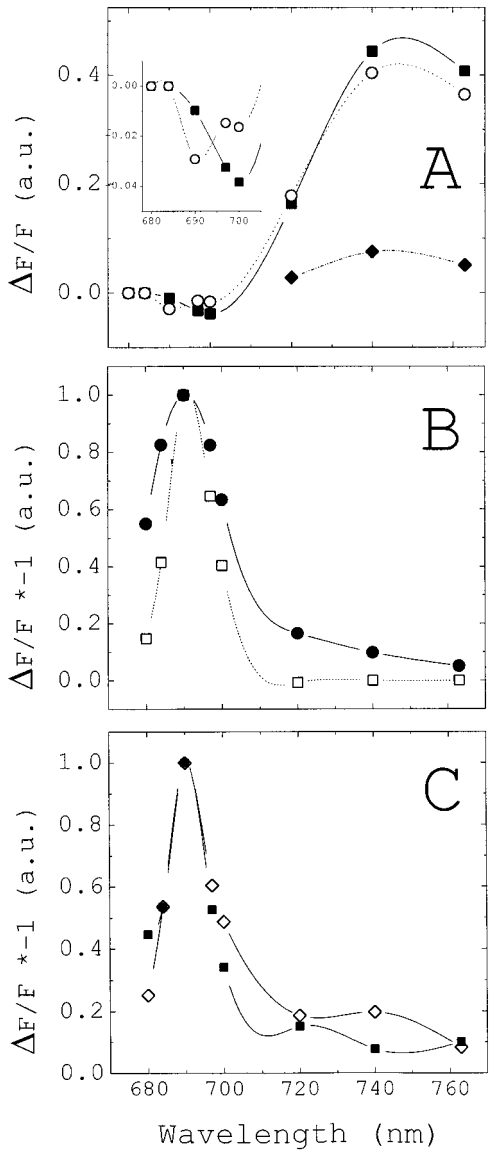

FIGURE 9: Microwave-induced fluorescence emission spectra of the triplet populations identified through global Gaussian deconvolution and the P_{680} recombination triplet. Panel A: Bands associated with PSI. Open circles and dotted line, 720/942 MHz triplet; solid squares and line, 733/951 MHz triplet; solid diamond and dash−dotted line, 757/972 MHz triplet. In the insert are shown in greater detail the spectra associated with $^3P_{700}$ in the wavelength region dominated by PSII emission. Panel B: Slow decaying (ms) PSII associated bands: Open squares and dashed line, 727/964 MHz triplet; solid circles and line, 741/972 MHz triplet. Panel C: the fast decaying (μs) PSII triplet population (766/989 MHz, open diamonds and solid line) and the P_{680} recombination triplet (721/991 MHz, solid squares and solid lines). To facilitate comparison, the amplitude values in panel B and C have been normalized at their maxima (690 nm).

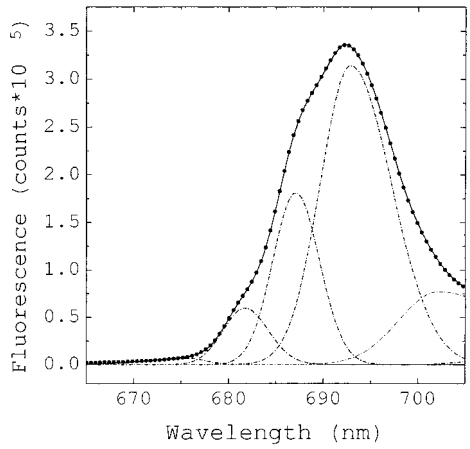

FIGURE 10: Deconvolution into Gaussian subbands of the fluorescence emission spectra of thylakoids in the 650−710 nm region (PSII associated emission) at 4.2 K. The points are the measured and smoothed emission spectrum recorded with an optical resolution of 0.5 nm. Dash−dotted lines are the Gaussian components and the solid line the fit function.

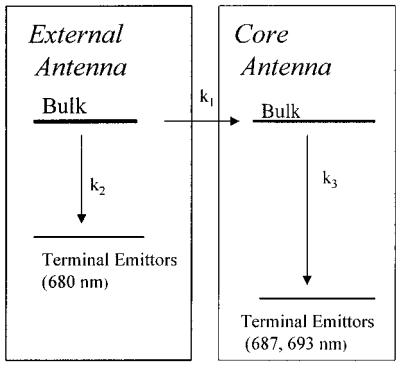

FIGURE 11: Kinetic scheme describing energy transfer at 2 K from the outer antenna of PSII to the terminal fluorescence emittors in both the core and outer antenna. k_1 is the rate constant for transfer from the outer antenna to the core antenna. k_2 and k_3 are the rate constants for transfer to the terminal emittors.

generated in complexes of the external antenna while the 766/989 and 727.7/964 MHz triplets are probably generated in the core complexes.

PSII Recombination Triplet. None of the triplet populations so far described correspond to the well-studied P_{680} recombination triplet (|D| − |E|, 720 MHz; |D| + |E|, 991 MHz). As it is thought that this triplet is important in photoinduced damage to PSII (*31*, *32*), we have examined whether its signal is induced by removing oxygen from the samples. This was achieved by dark incubation of thylakoids with 20 mM dithionite for 15 min at 4 °C and was found not to modify either the shape or the intensity of the FDMR spectra (data not presented). As oxygen is an efficient triplet quencher (*14*), this result is presumably due to its extremely low rate of diffusion at 1.8 K, the temperature at which measurements were made. Thus, even though Q_A is reduced under these conditions, the recombination triplet is not detectable. On the other hand, when the thylakoid membranes are incubated with 20 mM dithionite and illuminated with white light (2000 μE m^2 sec^{-1}) at room temperature, a signal with resonance frequency maxima at 720.5 MHz (|D| − |E|) and 991.0 MHz (|D| + |E|) appears at PSII detection wavelengths and progressively builds in with illumination time (Figure 12). This is the signal which has been attributed to the P_{680} recombination triplet (*44*), and it is seen to strongly overlap with the two shorter microwave PSII triplet populations. The ZFS parameters of this signal are |D| = 0.0285 cm^{-1} and |E| = 0.0045 cm^{-1} (Table 1). The zero-field splitting parameters of the P_{680} associated triplet are much closer to those of a Chl in which the central Mg ion is pentacoordinated than the other thylakoid triplets. It should be mentioned that this triplet is thought to reside on a monomer chlorophyll state closely associated with the primary donor (*30*, *52*−*56*) and oriented at about 30° to the plane of the membrane (*52*).

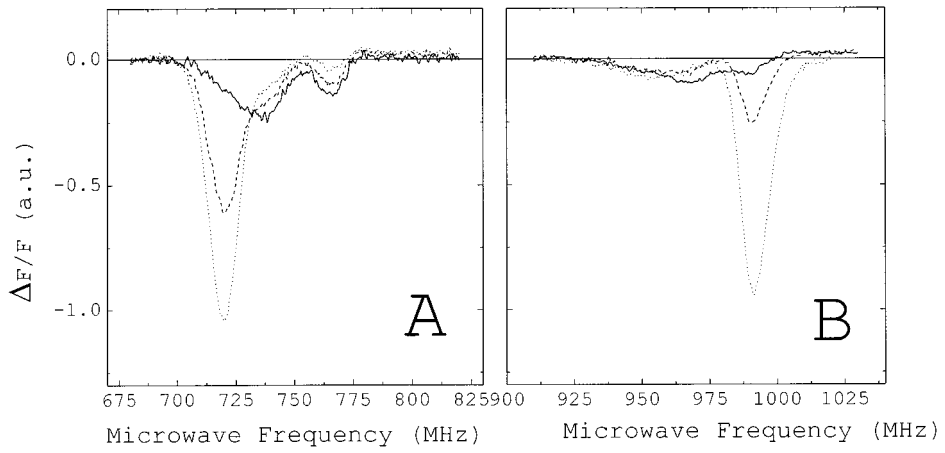

FIGURE 12: Effect of the preillumination time on the FDMR spectra of thylakoids which had been preincubated with 20 mM dithionite for 5min at 4 °C in the dark. Both the |D| − |E| (panel A**)** and |D| + |E| (panel B) Chl *a* resonance transitions are presented. Solid lines, control; dashed lines, 45 s; dotted lines, 150 s. λ_{em}, 690 nm (fwhm 10 nm); temperature, 1.8 K; Mw mod. freq., 33 Hz; lock-in ϕ, −105°; Mw power, 600 mW; scan rate, 5 MHz/sec.

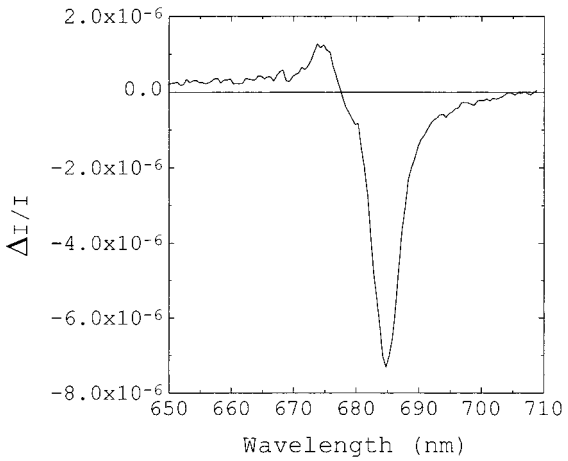

FIGURE 13: Triplet-minus-singlet spectrum of the Photosystem II reaction center recombination triplet in the Qy band of Chlorophyll, measured with a sample which had been incubated for 5 min in the dark at 4 °C with 20 mM dithionite and pre-illuminated for 6 min. Mw freq = 992 MHz, the maximum of the |D| + |E| transition. Optical resolution, 0.5 nm. Scan rate, 0.1 nm/sec; Mw power, 600 mW. Other conditions same as those in the legend of Figure 2.

In Figure 13, the microwave-induced T − S spectrum, obtained with a pump frequency of 992 MHz in the |D| + |E| transition, is presented. At this frequency and in the conditions of the experiments, the contribution of other triplet states to the T − S spectrum is certainly negligible. The main bleach is located at 685 nm, with a weak positive signal near 675 nm. Similar spectra are obtained with other pump frequencies within the |D| + |E| transition of this triplet (890−1010 MHz) (data not presented). This spectrum closely resembles those previously published by Carbonera et al. (*57*, *45*) though it is red shifted by about 0.5 nm. It is therefore evident that the triplet resides on the long-wavelength-absorbing chlorophyll state of the PSII reaction center complex, which is usually detected at 683−684 nm in absorption measurements of the isolated complex (*9*, *58*, *59*) but which is at 685 nm in the more intact thylakoid system. This is the pigment which Jankowiak and collaborators (*9*) have suggested may be a "linker chlorophyll" due to its proposed peripheral location in the D1·D2·Cytb_{559} complex and which would then correspond to either of the chlorophylls $ChlZ_{D1}$ or $ChlZ_{D2}$ in the crystallographic structure of Zouni et al. (*1*, *60*). The present data, together with previously published ADMR measurements (*8*, *57*), however clearly do not support this view, as these chlorophylls seem to be bound at about 30 Å from the central primary donor region, thus making the triplet transfer to them a low probability process, as this requires van der Waals contact. It therefore seems probable that the triplet is located on one of the four central chlorophylls, which according to the published crystal structure are within 10 Å (center to center) from each other with considerably smaller edge-to-edge distances.

As mentioned above, the present T − S spectra of the PSII recombination triplet is similar to those previously reported for relatively intact systems (*57*) but differs from those obtained with the isolated D1·D2·Cytb_{559} complex (e.g., *56*, *57*, *61*). These spectra show the maximum bleach at 680.6 nm, with a shoulder also present near 684 nm. The positive structure near 675 nm, present in our spectrum, is also present in those of the isolated reaction center complex. We therefore suggest that the difference encountered between the intact thylakoid system and that of the isolated D1·D2·Cytb_{559} complex is due to some pigment rearrangement which occurs during complex isolation. The minor structure present in the T − S spectrum of the isolated reaction center complex near 684 nm probably reflects the 685 nm band seen in our spectrum. On the basis of optical spectra of isolated reaction center with modified pheophytin at 6 K, Germano et al. (*56*) have suggested that the triplet state in the PSII reaction center complex is localized on the Chl corresponding to B_A in purple bacteria, while the shoulder at about 684 nm could be due to excitonic interaction. The present data for thylakoids which have a main bleach at 685 nm and only a small negative contribution at 680 nm do not seem in agreement with this suggestion that this band is primarily excitonic in nature.

In the crystallographic structure of the PSII reaction center, the four central chlorophylls have a center-to-center distance of about 10 Å. Thus, they are sufficiently close for Coulombic interactions (greater than 100 cm^{-1}) to be established between the singlet states, depending on the orientation of the transition dipole moments. Such interactions, which

would give rise to excitonic band splitting and redistribution of dipole oscillator strength, will be broken when a triplet is formed, and this should lead to a redistribution of oscillator strength as well as band shifts. The absence of major changes in the T − S spectrum outside the band peaking at 685 nm indicates that the Chl_{685} may be considered to be predominately monomeric. This interpretation is in agreement with previous studies on the selective photooxidation of the long wavelength pigment in the isolated reaction center complex at 77 K (*59*), where only a minor change in the 675 nm region accompanied oxidation of the 683 nm absorbing pigment.

FURTHER DISCUSSION

The triplet state of Chl is of physiological importance because of its interaction with the ground state of dioxygen, and the consequent generation of the extremely reactive oxygen singlet species, capable of damaging most biological compounds (*14*). A putative central role for the P_{680} recombination triplet in the PSII light-induced loss of photochemical activity, a phenomenon known as photoinhibition, has been proposed by many laboratories (*31*, *32*). Previous experiments, originally performed by conventional EPR and confirmed with zero-field ODMR technique, have demonstrated that the P_{680} triplet is populated upon double reduction and protonation to a neutral form of the primary quinone acceptor. In the present study, we have detected the presence of at least three different triplet populations for PSII, but none of these in the untreated thylakoid membrane could be assigned to the PSII recombination triplet on the basis of the ZFS parameters, even in strongly reducing conditions. The fast decaying triplet (766/989 MHz) is probably located on a Chl population, close to the reaction center, as is the 727/964 MHz triplet, while the 741/972 MHz triplet may be generated by external antenna complex(es). It should be pointed out that while FDMR is a highly sensitive technique, it is not possible to use it to determine triplet yields. Thus, we are unable to comment on the yields of these three triplet states associated with PSII. It should, however, be underlined that, under the same measuring conditions, these three triplets are present at detectable levels while that of the P_{680} recombination triplet is not. We therefore think it highly probable that they may be involved in photoinhibition of PSII at physiological temperatures. This suggestion is in line with recently determined action spectra of photoinhibition which point to the involvement of both external and core antenna complexes (*62*).

ACKNOWLEDGMENT

We are thankful to Prof. F. Garlaschi for the help in low-temperature fluorescence measurements and to Prof. G. Giacometti and Dr. G. Agostini for constant support and interest in the ODMR measurements. We also acknowledge Prof. G. M. Giacometti for the use of laboratory equipment during sample preparation.

REFERENCES

1. Zouni, A., Witt, H. T., Kern, J., Fromme, P., Krauss, N., Saenger, W., and Orth, P. (2001) *Nature 408*, 739−743.
2. Schubert, W. D., Klukas, O., Krauss, N., Saenger, W., Fromme, P., and Witt, H. T. (1997) *J. Mol. Biol. 272*, 741−69.
3. Klukas, O., Schubert, W. D., Jordan, P., Krauss, N., Fromme, P., Witt, H. T., and Saenger, W. (1999) *J. Biol. Chem. 274*, 7361−7367.
4. Bottcher, B., Graber, P., and Boekema, E. J. (1992) *Biochim. Biophys. Acta 1100*, 125−136.
5. Rhee, K. H., Morris, E. P., Zheleva, D., Hankamer, B., Kuhlbrandt, W., and Barber, J. (1997) *Nature 389*, 522−526.
6. Morris, E. P., Hankamer, B., Zheleva, D., Friso, G., and Barber, J. (1997) *Structure 5*, 837−849.
7. Den Blanken, H. J., and Hoff, A. J. (1983) *Biochim. Biophys. Acta 724*, 52−61.
8. Den Blanken, H. J., Hoff, A. J., Jongenelis, A. P. J. H., and Diner, B. (1983) *FEBS Lett. 157*, 21−27.
9. Jankowiak, R., Ratsep, M., Picorel, R. Seibert, M., and Small, G. J. (1999) *J. Phys. Chem. B 103*, 9759−9769.
10. Tetenkin, V. L., Gulyaev, B. A., Seibert, M., and Rubin, A. B. (1989) *FEBS Lett. 250*, 459−463.
11. Durrant, J. R., Hastings, G., Joseph, D. M., Barber, J., Porter, G., and Klug, D. R. (1992) *Proc. Natl. Acad. Sci. U.S.A. 89*, 11632−11636.
12. Jennings, R. C., Bassi, R., and Zucchelli, G. (1994) *Top. Curr. Chem. 1*, 148−181.
13. Krasnowsky, A. A. (1982) *Photochem. Photobiol. 36*, 733−741.
14. Krasnowsky, A. A. (1994) *Biophysics 39*, 197−211.
15. Kramer, H., and Mathis, P. (1980) *Biochim. Biophys. Acta 593*, 319−29.
16. Wolff, C., and Witt, H. T. (1969) *Z. Naturfosch. 24b*, 1031−1037.
17. Mathis, P., Butler, W. L., and Satoh, K. (1979) *Photochem. Photobiol. 30*, 603−614.
18. van der Vos, R., Carbonera, D., and Hoff, A. J. (1991) *Appl. Magn. Reson. 2*, 179−202.
19. Schodel, R., Irrgang, K. D., Voigt, J., and Renger, G. (1998) *Biophys. J. 75*, 3143−3153.
20. Carbonera, D., Giacometti, G., Agostini, G., Angerhofer, A., and Aust, V. (1992) *Chem. Phys. Lett. 194*, 275−281.
21. Peterman, E. J. G., Dekker, J., van Grondelle, R., and van Amerongen, H. (1995) *Biophys. J. 69*, 2670−2678.
22. Barzda, V., Peterman, E. J. G., van Grondelle, R., and van Amerongen, H. (1998) *Biochemistry 37*, 546−551.
23. Carbonera, D., Giacometti, G., and Agostini, G. (1992) *Appl. Magn. Reson. 3*, 361−368.
24. Groot, M.-L., Peterman, E. J. G., van Stokkum, I. H. M., Dekker, J. P., and van Grondelle, R. (1995) *Biophys. J. 68*, 281−290.
25. Bearden, R., and Malkin, R. (1972) *Biochim. Biophys. Acta 283*, 456−468.
26. Shuvalov, V. A. (1976) *Biochim. Biophys. Acta 430*, 113−121.
27. Frank, H. A., McClean, M. B., and Sauer, K. (1979) *Proc. Natl. Acad. Sci. U.S.A. 76*, 5124−5128.
28. Setif, P., Bottin, H., and Mathis, P. (1985) *Biochim. Biophys. Acta 808*, 112−122.
29. Rutherford, W. A., and Mullet, J. E. (1981) *Biochim. Biophys. Acta 636*, 225−235.
30. van Mieghem, F. J. E., Nitschke, W., Mathis, P., and Rutherford, W. A. (1989) *Biochim. Biophys. Acta 977*, 207−214.
31. Durrant, J. R., Giorgi, L. B., Barber, J., Klug, D. R., and Porter, G. (1990) *Biochim. Biophys. Acta 1017*, 167−175.
32. Vass, I., and Styring, S. (1993) *Biochemistry 32*, 3334−3341.
33. Santabarbara, S., Garlaschi, F. M., Zucchelli, G., and Jennings, R. C. (1999) *Biochim. Biophys. Acta 1409*, 165−170.
34. Santabarbara, S., Neverov, K., Garlaschi, F. M., Zucchelli, G., and Jennings, R. C. (2001) *FEBS Lett. 491*, 109−113.
35. Tyystjarvi, E., King, N., Hakala, M., and Aro, E.-M. (1999) *J. Photochem. Photobiol., B 48*, 142−147.
36. Jennings, R. C., Garlaschi, F. M., Gerola, P. D., Etzion-Katz, R., and Forti, G. (1981) *Biochim. Biophys. Acta 638*, 100−107.
37. MacKinney, G. (1941) *J. Biol. Chem. 140*, 315−322.
38. Zucchelli, G., Jennings, R. C., and Garlaschi, F. M. (1990) *J. Photochem. Photobiol., B 6*, 381−394.
39. Schweitzer, R. H., and Brudvig, G. W. (1997) *Biochemistry 36*, 11351−11359.
40. Siffel, P., Hunova, I., and Rohacek, K. (2000) *Photosynth. Res.* 6, 219−229.
41. Zucchelli, G., Garlaschi, F. M., and Jennings, R. C. (1996) *Biochemistry 35*, 16247−16254.
42. Searle, G. F. W., Koehorst, R. B. M., Schaafsma, T. J., Moller-Linderg, B., and VonWettstein, D. (1981) *Carslberg Res. Commun. 46*, 183−194.

43. Searle, G. F. W., and Schaafsma, T. J. (1992) *Photosynth. Res. 32*, 93−206.
44. Carbonera, D., DiValentin, M., Giacometti, G., and Agostini, G. (1994) *Biochim. Biophys. Acta 1185*, 167−176.
45. Carbonera, D., Collareta, P., and Giacometti. G. (1997) *Biochim. Biophys. Acta 1322*, 115−128.
46. Mathis, P., Saar, K., and Remy, R. (1978) *FEBS Lett. 88*, 275−278.
47. Hoff, A. J. (1995) in *Advances in Photosynthesis* (Amesz, J., and Hoff, A. J., Eds.) Vol. 3, *Biophysical Techniques in Photosynthesis*, pp 277−298, Kluwer Academic Publisher, Dordrecht, The Netherlands.
48. Budil, D. E., and Thurnauer, M. C. (1991) *Biochim. Biophys. Acta 1057*, 1−41.
49. Rijgersberg, C. P., Amesz, J., Thielen, A. P. G. M., and Swager, J. A. (1979) *Biochim. Biophys. Acta 54*, 473−482.
50. Tang, D., Jankowiack, R., Seibert, M., Yochum, C. F., and Small, G. (1990*) J. Phys. Chem. B 94*, 6519−6522.
51. Jankowiak, R., Zazubovich, V., Ratsep, M., Matsuzaki, S., Alfonso, M., Picorel, R., Seibert, M., and Small, G. J. (2000) *J. Phys. Chem. B 104*, 11805−11815.
52. van Mieghem, F. J. E., Satoh, K., and Rutherford, A. W. (1991) *Biochim. Biophys. Acta 1058*, 379−385.
53. Rutherford, A. W. (1986) *Biochem. Soc. Trans. 14*, 15−17.
54. Noguchi, T., Tomo, T., and Inoue, Y. (1998) *Biochemistry 37*, 13614−13625.
55. Noguchi, T., Tomo, T., and Kato, C. (2001) *Biochemistry 40*, 2127−218558.
56. Germano, M., Shkuropatov, A. Y.; Permentier, H; de Wijn, R.; Hoff, A. J., Shuvalov, V. A., and van Gorkom, H. J. (2001) *Biochemistry 40*, 11472−11482.
57. Carbonera, D., Giacometti, G., and Agostini, G. (1994) *FEBS Lett. 343*, 200−204
58. Otte, S. C. M., Van der Vos, R., and van Gorkom, H. J. (1992) *J. Photochem. Photobiol., B 15*, 5−14.
59. Finzi, L., Elli, G., Zucchelli, G., Garlaschi, F. M., and Jennings, R. C. (1998) *Biochim. Biophys. Acta 1366*, 256−264.
60. Vassil'ev, S., Orth, P., Zouni, A., Owens, T. G., and Bruce, D. (2001) *Proc. Natl. Acad. Sci. U.S.A. 98*, 8602−8607.
61. Kwa, S. L. S., Eijckelohoff, C., van Grondelle, R., and Dekker, J. P. (1994) *J. Phys. Chem. 98*, 7702−7711.
62. Santabarbara, S., Cazzalini, I., Rivadossi, A., Garlaschi, F. M., Zucchelli, G., and Jennings, R. C. (2002) *Photochem. Photobiol*., in press.

BI0201163